Heliyon 10 (2024) e28580

Contents lists available at ScienceDirect

Heliyon

journal homepage: www.cell.com/heliyon

Research article

Prognostic effect of DNA methylation of *BTG2* gene in Chinese hepatocellular carcinoma

Jungang Ma [a,1], Zhuo Chen [a,1], Shuixia Liu [b], Chuan Chen [a], Wei Guan [a], Mingying Geng [a], He Xiao [a], Bijing Mao [c,**], Bin Wang [d,*]

[a] *Department of Oncology, Daping Hospital, Army Medical University, Chongqing, 400042, China*
[b] *Department of Ophthalmology, Daping Hospital, Army Medical University, Chongqing, 400042, China*
[c] *Department of Oncology, The Third Affiliated Hospital of Chongqing Medical University, Chongqing, 401120, China*
[d] *Department of Oncology, The Seventh People's Hospital of Chongqing (Affiliated Central Hospital of Chongqing University of Technology), Chongqing, 400054, China*

ARTICLE INFO

Keywords:
Hepatocellular carcinoma
DNA methylation
B-cell translocation gene 2
Prognosis

ABSTRACT

Background: This study aims to develop a prognostic model for overall survival based on potential methylation sites within B-cell translocation gene 2 (*BTG2*) in Chinese patients with hepatocellular carcinoma (HCC).

Methods: This is a retrospective study. The beta values of nine CpG sites and RSEM normalized count values of *BTG2* gene were extracted from the Cancer Genome Atlas-Liver Hepatocellular Carcinoma (TCGA-LIHC) (TCGA-LIHC) dataset, with the beta value representing the methylation level by indicating the ratio of the intensity of the methylated bead type to the combined locus intensity. Pyrosequencing was performed to determine the range of methylation values surrounding cg01798157 site in *BTG2* gene. A weighted linear model was developed to predict the overall survival (OS).

Results: The beta value of cg01798157 was significantly negatively associated with the mRNA expression of *BTG2* in the TCGA-LIHC dataset (Spearman's rho = −0.5306, $P = 2.27 \times 10^{-27}$). The methylation level of cg01798157 was significantly associated with OS in the cohort of 51 Chinese HCC patients (Hazard ratio = 0.597, 95% CI: 0.434–0.820, $P = 0.001$). Multivariate Cox regression analysis identified methylation level of cg01798157, cirrhosis, and microvascular invasion as independent prognostic factors. The prognostic efficiency of death risk score was superior to that of cirrhosis or microvascular invasion alone.

Conclusions: The methylation level of cg01798157 in *BTG2* may be an epigenetic biomarker in Chinese patients with resectable HCC.

* Corresponding author. Department of Oncology, The Seventh People's Hospital of Chongqing (Affiliated Central Hospital of Chongqing University of Technology), Lijiatuo Street, Chongqing, 400054, China.
** Corresponding author. Department of Oncology, The Third Affiliated Hospital of Chongqing Medical University, 1 Shuanghu Branch Road, Yubei District, Chongqing, 401120, China.
E-mail addresses: 651124@hospital.cqmu.edu.cn (B. Mao), wangjianlinbin@163.com (B. Wang).
[1] These authors are equally contributed to this study.

https://doi.org/10.1016/j.heliyon.2024.e28580
Received 5 August 2023; Received in revised form 19 March 2024; Accepted 20 March 2024

1. Background

Hepatocellular carcinoma (HCC) accounts for 85–90% of primary liver cancer and carries significant cancer-related morbidity and mortality worldwide [1,2]. Approximately half of the worldwide cases of HCC occur in China. The major risk factors for HCC include hepatitis B virus (HBV)/hepatitis C virus (HCV) infection, heavy alcohol consumption, and exposure to dietary toxins such as aflatoxin and aristolochic acid. All these risk factors are potentially preventable, and by risk factor management, the incidence HCC in China has decreased by 20% in the past two decades [3]. In early stage HCC, surgical resection can bring promising survival benefits with the 5-year overall survival (OS) rate approaching 70% [4], whereas the majority of HCC patients is diagnosed at unresectable stages. Despite the significant progress in comprehensive treatment for unresectable HCC, the prognosis remains dismal with the 1-year OS rate less than 70% [5]. Moreover, about 50% of HCC patients develop disease recurrence or distant metastasis after surgical resection with the median survival less than 2 years [6]. Therefore, there is an urgent need to find new therapeutic targets or biomarkers for prognosis prediction, which can in turn provide clues for the development of individualized therapy for HCC.

Emerging evidence has highlighted the significance of genome, transcriptome, and epigenetics biomarkers for the risk stratification of local recurrence and distant metastasis of HCC [7–9]. However, these multi-omics studies fail to demonstrate targetable mutations that can be used for the treatment of HCC. DNA methylation, an epigenetic modification [7,10], occurs earlier and is constant during tumorigenesis compared with gene mutation. Aberrant alternations in DNA methylation are important prognostic hallmarks for lung cancer [11], breast cancer [12], and esophageal cancer [13]. Multi-omics analysis of HCC has demonstrated that 53% of HCC patients have epigenetic silencing of CDKN2A gene caused by DNA methylation, while merely 4% have CDKN2A gene mutation among these patients, suggesting that DNA methylation is the primary mechanism responsible for gene inactivation [7]. The prognostic role of DNA methylation in HCC has been well-documented [14,15]. These studies suggest that DNA methylation, as a potential therapeutic target for HCC, warrants more in-depth exploration.

B-cell translocation gene 2 (*BTG2*), also known as PC3/TIS21, is the firstly identified gene in the TOB/BTG family, which is located in chromosome 1q32.1 and encodes a 158 amino acid protein [18]. *BTG2* has been reported to act as a tumor suppressor in human malignancies [16,17]. *BTG2* is poorly expressed in various cancers including lung cancer [19], prostate cancer [20], and breast cancer [21]. The decrease in *BTG2* expression is indicative of poor prognosis in cancer patients. Our previous studies have found that *BTG2* gene expression is down-regulated in HCC, and patients with lower expression of *BTG2* have shorter OS [22]. However, the prognostic significance of DNA methylation of *BTG2* in HCC has not been reported yet.

This study aimed to analyze the prognostic role of DNA methylation of *BTG2* gene in HCC by screening functional methylation sites of *BTG2*. Firstly, CpG sites with the highest correlation with *BTG2* mRNA were selected from the Cancer Genome Atlas-Liver Hepatocellular Carcinoma (TCGA-LIHC) (TCGA-LIHC) database, and then, paraffin samples of HCC cohort from the Seventh People's Hospital of Chongqing were collected for pyrosequencing to evaluate the prognostic significance of selected CpG sites on the OS of HCC patients. Finally, our findings underscore that the addition of CpG methylation status can improve the prognostic ability of routine clinical prognostic indicators for OS in HCC patients, which indicates that DNA methylation of *BTG2* can be used as a new prognostic marker for HCC.

2. Methods

2.1. TCGA-LIHC datasets and data extraction

Preprocessed methylation dataset of liver cancer (Dataset ID: TCGA. LIHC.sampleMap/HumanMethylation450 version. 2017-09-08) was downloaded from UCSC (https://xenabrowser.net/datapages/). The TCGA-LIHC dataset contains DNA methylation profiles of 429 tissue samples from patients with HCC. The deposited DNA methylation profile was previously measured through the Illumina Infinium HumanMethylation450 platform. The methylation level was represented by the beta value, which is defined as the ratio of the intensity of the methylated bead type to the combined locus intensity. The Illumina methylation analyzer (IMA) in the R package was used to extract CpG sites within *BTG2* gene and corresponding beta values. All CpG probe sites within *BTG2* gene were obtained by setting "UCSC_REFGENE_NAME" to "*BTG2*" in the annotation file "fullannoInd". However, beta values were finally retrieved from only nine CpG probes. The *BTG2* mRNA expression data of 423 tissue samples in the form of $\log_2$ (x+1) transformed from RNA-Seq by expectation-maximization (RSEM) were downloaded from UCSC (https://xenabrowser.net/datapages/). In the format of $\log_2$ (x+1), the x is RSEM. After merging the beta values and mRNA expression data by sample identifiers, we obtained a total of 371 cases eligible for evaluating the association between beta value (DNA methylation) and *BTG2* mRNA expression.

2.2. Patient characteristics and follow up

A total of 51 Chinese patients with HCC confirmed by pathological diagnosis and treated at the Seventh People's Hospital of Chongqing from January 2012 to December 2014 were randomly enrolled. All patients were diagnosed with primary liver cancer and eligible for complete resection. According to the grading system of World Health Organization (WHO), 5 cases presented with well differentiated carcinomas, 37 cases with moderately differentiated carcinomas, and 9 cases with poorly differentiated carcinomas. Based on the latest clinical data before surgical resection, the liver function of HCC patients was evaluated using the Child-Pugh classification method, with 46 cases classified as Child-Pugh A and 6 cases classified as Child-Pugh B or C. Exclusion criteria were as follows: preoperative radiotherapy or chemotherapy, unable to receive radical resection due to preoperative diagnosis of distant metastasis, positive surgical margin, or unconventional treatment. The median follow-up time was 25 months (range: 2.00–52.0

months). Patients were followed up through telephone interviews. Overall survival (OS) was defined as the time from surgery to the date of death or the last follow-up. The study procedures were approved by the Human Ethics Committee of the Daping Hospital (Oct 2020), and all patients signed the informed consent form for the collection of tissue samples and clinical data. This is a retrospective study, and the personal privacy information of all patients were de-identified.

2.3. Pyrosequencing

The tissue samples obtained via complete tumor resection were fixed with 10% formalin, embedded in paraffin, and cut into 10 μm sections. Genomic DNA was extracted from 10 sections using the QIAamp DNA FFPE Tissue Kit (QiaGen, Hilden, Germany). The concentration and purity of these DNA samples were determined with a spectrophotometer (NanoDrop2000, Thermo Scientific, Waltham, MA, USA). Totally 500 ng of purified DNA in each sample was subjected to bisulfite conversion with EZ DNA Methylation-GoldTM Kit according to manufacturer's instructions (Cat. No. D5006, Zymo Research Corporation, Orange, CA, USA). The bisulfite conversed DNA was amplified with TaKaRa EpiTaqTM HS (Cat. No. R110A, Takara Biomedical Technology (Beijing) Co., Ltd. Beijing, China) with the reaction setup: 10 ng bisulfite-treated DNA, 0.4 μM forward and reverse primers, 2.5 μL 10 × EpiTap PCR Buffer, 2.5 mM $MgCl_2$, dNTP Mixture (0.264 mM each), and EpiTap HS (0.025 U/μL) in total 25 μL each reaction. A typical PCR reaction was performed by 35 thermic cycles of denaturation at 98 °C for 10 s, annealing at 55 °C for 30 s, and extension at 72 °C for 30 s, followed by extension at 72 °C for 1 min and maintaining at 4 °C. The amplicons were then subjected to pyrosequencing with PyroMark Q96 (QiaGen, Hilden, Germany). The primer sequences: forward 5′-AGGTATGTGGTGGTTTGTTG-3′ and reverse 5′- TCCTCACCTA-CAAAAACCAAATACTACTA-3′. The polymerase chain reaction products underwent pyrosequencing with the specific probes: 5′-ACTACCTAATAACAATCTCCAACTA-3′.

2.4. Statistical analysis

In TCGA LIHC data set, the association between beta value and *BTG2* mRNA expression was determined using Spearman's rank correlation coefficient, which was denoted as "Spearman's rho" in the current study.

To demonstrate that the methylation level within the promoter region of the *BTG2* gene could provide additional prognostic information beyond clinical factors, a two-stage prognostic analysis was conducted. In the first stage, independent prognostic factors for overall survival (OS) were identified among the clinical factors in the cohort [23]. Univariate Cox regression was first utilized for each individual clinical factor. The hazard ratio (HR) represents the ratio of hazard rates between two groups. Subsequently, a stepwise Cox regression was employed to determine the independent prognostic factors among the candidates that exhibited a P-value of <0.05 on univariate Cox regression. Candidate variables were selected based on the likelihood ratio test for inclusion ($P < 0.05$) and exclusion ($P < 0.15$). In the second stage, the significance of adding the methylation level of cg01798157 to the identified clinical prognostic factors was evaluated using multivariate Cox regression. A prognostic score was defined as the sum of clinical characteristics and the methylation level of the *BTG2* gene, weighted with the corresponding coefficients from the multivariate Cox regression.

The accuracy of cirrhosis, microvascular invasion, methylation level of the *BTG2* gene, and the prognostic score for OS prognosis was determined using the c-index, calculated with the "concordance.index" function in the R package "survcomp" (version 1.48.0). The time-dependent receiver operating characteristic (ROC) curve was drawn by the "timeROC" package to estimate the accuracy of 1-year and 2-year OS prediction. Two time-dependent areas under the curve (AUC) were compared with function "compare" embedded in the R package "timeROC" (version 0.3 published in 2015-03-25). Benjamini-Hochberg method was used to correct false-positive discovery in the situation of multiple comparisons. Function "xyplot" and "corrplot" in the R package "lattice" were used to generate scatter plot and correlation map, respectively. All other statistical analyses were performed using SPSS 17.0 (IBM SPSS, Chicago, IL, USA). All tests were bilateral, and $P < 0.05$ was considered statistically significant. We reported this study following the Reporting Recommendations for Tumor Marker Prognostic Studies (REMARK) guidelines [24].

3. Results

The beta value of CpG sites within BTG2 gene were significantly negatively associated with mRNA expression.

Table 1
Spearman correlation coefficients between mRNA expression level and beta values in nine CpG sites in TCGA LICA dataset (n = 371).

	Median (range)	*Spearman's rho*	*P* value	Adjusted *P*
BTG2_mRNA	9.396 (6.497–13.761)			
cg01798157	0.837 (0.047–0.950)	−0.5306	2.52×10^{-28}	2.27×10^{-27}
cg23371584	0.222 (0.030–0.931)	−0.3102	1.02×10^{-9}	4.59×10^{-9}
cg00567854	0.784 (0.267–0.914)	−0.2855	2.17×10^{-8}	6.51×10^{-8}
cg02299360	0.088 (0.047–0.706)	−0.2457	1.67×10^{-6}	3.76×10^{-6}
cg06373167	0.696 (0.091–0.934)	−0.2062	6.32×10^{-5}	0.0001
cg12586428	0.013 (0.009–0.023)	0.0917	0.0779	0.1168
cg20138067	0.646 (0.216–0.886)	−0.0867	0.0955	0.1229
cg24337809	0.048 (0.026–0.391)	−0.0669	0.1988	0.2236
cg10935550	0.046 (0.025–0.277)	0.0602	0.2471	0.2471

In the 371 HCC cases from the TCGA-LIHC dataset, the beta value of cg01798157 (Spearman's rho = −0.5306, adjusted $P = 2.27 \times 10^{-27}$) was significantly negatively associated with *BTG2* mRNA expression, followed by cg23371584 (Spearman's rho = −0.31, adjusted $P = 4.59 \times 10^{-9}$) (Table 1 and Fig. 1). In contrast, the beta values of cg12586428, cg10935550, and cg24337809 remained consistently low in patients and were not associated with *BTG2* mRNA expression (Fig. 1). The distribution of all CpG sites detected by Pyrosequencing was shown in Fig. 2.

3.1. Prognostic role of cg01798157 methylation level

The baseline clinicopathological characteristics of the HCC cohort were shown in Table 2. Conveniently, pyrosequencing allowed for all CpG sites surrounding cg01798157 within the primers to be sequenced simultaneously. As evidenced by Spearman's rank correlation coefficient, each pair of CpG sites was highly correlated (Fig. 2). All other CpG sites were strongly positively correlated with cg01798157 (Spearman's rho ranges from 0.83 to 0.95) (Fig. 3).

Univariate Cox regression revealed that liver cirrhosis, Child-Pugh score, microvascular invasion, and methylation level of cg01798157 were all correlated with OS of HCC patients (Table 3, Fig. 4A and B). However, among the clinical factors found to be significantly associated with OS in the univariate Cox regression, only cirrhosis (Yes vs. No, HR = 8.744, 95% CI: 1.164–65.697, P = 0.035) and microvascular invasion (Yes vs. No, HR = 3 0.896, 95% CI: 1.332–11.396, P = 0.013) were identified as independent prognostic factors for OS through stepwise Cox regression. In multivariate Cox regression, it is clearly shown that after adjusting for cirrhosis and microvascular invasion, the methylation level of cg01798157 remained a significant prognostic factor for HCC OS (HR = 0.555, 95% CI: 0.399–0.771, $P < 0.001$) (Table 4).

3.2. Development of prognostic score for OS

Multivariate Cox regression shown in Table 4 was used to calculate the prognostic score by the following formula: 2.365 × cirrhosis (0 or 1) + 1.458 × microvascular invasion (0 or 1) −0.059 × methylation level of cg01798157 (continuous variable). The median value of prognostic score in the whole cohort was −1.816 (range: −4.917 to 3.058). Patients were stratified into the low-risk group and high-risk group according to the median value of prognostic score. The 1-year OS rate in the low-risk and high-risk groups were 83.89% and 39.86%, respectively (Log rank $P < 0.001$) (Fig. 4C). Moreover, the prognostic score (HR = 3.135, 95% CI: 1.797–5.468, $P <$

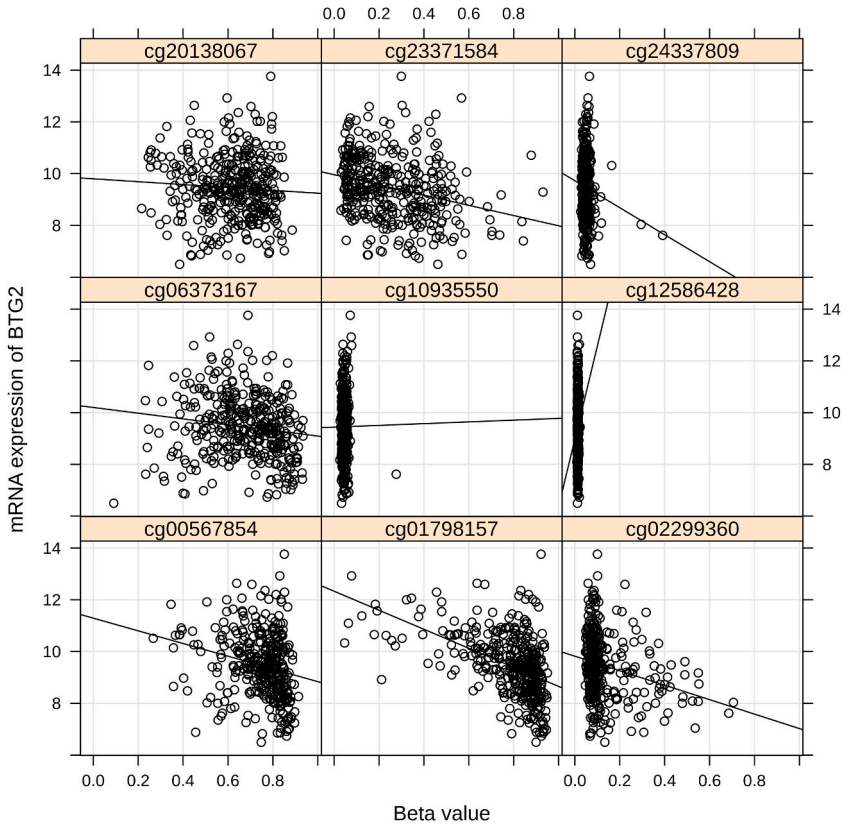

Fig. 1. Scatter plots showing correlation between methylation level of each CpG site and mRNA expression of *BTG2*. The straight line in each panel is a linear regression line.

Fig. 2. Diagram showing CpG distribution within 3′-UTR of *BTG2* gene. The cg01798157 and other 5 CpG sites detected by pyrosequencing are highlighted in the red characters.

Table 2
Baseline characteristics of 51 HCC cases cohort.

Characteristics		n (%)/Median (range)
Sex	Male	46 (90.2)
	Female	5 (9.8)
Age	≤52	24 (47.1)
	>52	27 (52.9)
Differentiation	Well	5 (9.8)
	Moderate	37 (72.5)
	Poor	9 (17.6)
Diameter of tumor	≤5	24 (47.1)
	>5	27 (52.9)
Cirrhosis	Yes	37 (72.5)
Hepatitis B	Yes	38 (74.5)
AFP	≤20	20 (39.2)
	>20	31 (60.8)
Child-Pugh	A	45 (88.2)
	B or C	6 (11.8)
Setallite	Yes	0 (0.0)
Portal vein thrombosis	Yes	6 (11.8)
Intrahepatic metastasis	Yes	5 (9.8)
BTG2 CpG_1		79 (32–94)
BTG2 CpG_2		79 (28–94)
BTG2 CpG_3		67 (25–85)
BTG2 CpG_4		73 (24–92)
cg01798157		64 (21–87)
BTG2 CpG_5		69 (24–90)

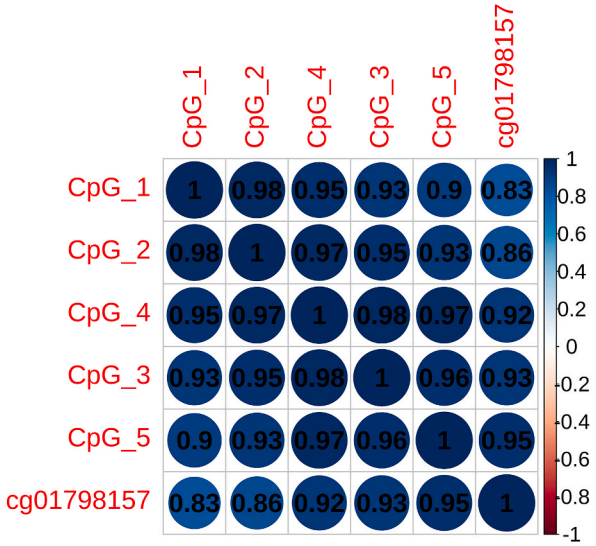

Fig. 3. Correlation coefficient plot of CpG sites surrounding cg01798157 in *BTG2* 3′-UTR.

0.001) was significantly associated with OS after adjusting for gender, age, tumor differentiation, tumor size, hepatitis, Child-Pugh score, and alpha-fetoprotein (AFP).

The c-index values for cirrhosis, microvascular invasion, methylation level of the *BTG2* gene, and the prognostic score were 0.894

Table 3
Univariate Cox regression for OS in the validation set (n = 51).

Factors	Univariate	
	HR (95% CI)	*P*
Sex (Female vs Male)	0.873 (0.202–3.771)	0.856
Age (>52 vs ≤52)	0.939 (0.390–2.258)	0.888
Differentiation (Moderate vs Well)	0.566 (0.156–2.046)	0.385
Differentiation (Poor vs Well)	1.475 (0.368–5.913)	0.583
Diameter of tumor (>5 vs ≤5)	0.777 (0.319–1.889)	0.577
Cirrhosis (Yes vs No)	9.629 (1.282–72.039)	0.027
Hepatitis B (Yes vs No)	3.126 (0.722–13.529)	0.127
AFP (>20 vs ≤20)	2.744 (0.989–7.617)	0.053
Child-Pugh (B/C vs A)	3.214 (1.048–9.860)	0.041
Portal vein thrombosis (Yes vs No)	4.653 (1.584–13.668)	0.005
Intrahepatic metastasis (Yes vs No)	1.240 (0.286–5.378)	0.774
cg01798157	0.597 (0.434–0.820)[a]	0.001

[a] The HR and 95% CI was calculated based on per 10% increment in beta value.

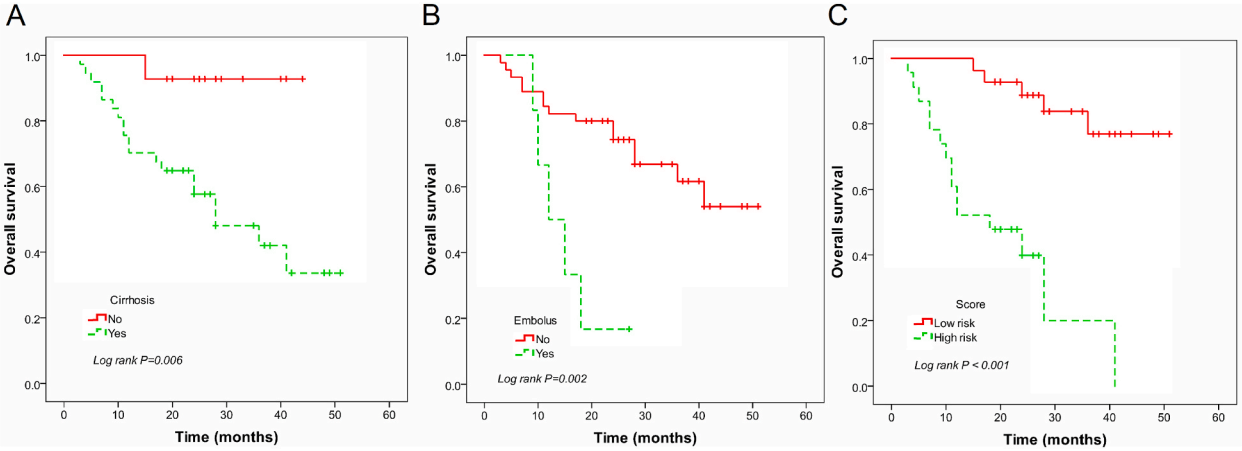

Fig. 4. Kaplan-Meier curves illustrating significant differences in prognosis between patients with or without cirrhosis [a], with or without microvascular invasion [b], and with high or low risk score [c].

Table 4
Final weighted linear model for prognosis of OS.

	β	S.E.	HR (95% C·I.)	*P*
Cirrhosis (Yes vs No)	2.365	1.033	10.64 (1.405–80.636)	0.022
Portal vein thrombosis (Yes vs No)	1.458	0.563	4.299 (1.426–12.955)	0.010
cg01798157	−0.059	0.017	0.555 (0.399–0.771)[a]	0.000

[a] The HR and 95% CI was calculated based on per 10% increment in beta value.

Table 5
Comparison of AUCs from the results of time-dependent ROC analysis to evaluate accuracies of Cirrhosis, Portal vein thrombosis, cg01798157 and Score to predict prognosis of OS.

Factors	AUC (95% CI) at 1 year	AUC (95% CI) at 2 year	*P* value compared with Score at 1 year	*P* value compared with Score at 2 year
Cirrhosis (Yes vs No)	0.675 (0.600–0.750)	0.664 (0.546–0.783)	1.21×10^{-6}	3.67×10^{-4}
Portal vein thrombosis (Yes vs No)	0.574 (0.430–0.717)	0.659 (0.526–0.791)	4.01×10^{-7}	5.66×10^{-4}
cg01798157	0.869 (0.751–0.988)	0.777 (0.622–0.932)	0.4381971	0.0821
Score	0.919 (0.839–0.999)	0.904 (0.809–0.999)		

(95% CI: 0.711–1.000), 0.809 (95% CI: 0.688–0.929), 0.703 (95% CI: 0.605–0.802), and 0.817 (95% CI: 0.755–0.878) respectively. There were no significant differences between the prognostic score compared with cirrhosis and microvascular invasion (P = 0.894 and 0.441 respectively). However, the c-index of the prognostic score was higher than that of the methylation level of the *BTG2* gene (P = 0.004). Time-dependent ROC analysis revealed that the prognostic score had the largest AUC for predicting 1-year and 2-year OS (Table 5, Fig. 5A, B). The AUC of prognostic score was significantly higher than that of cirrhosis and microvascular invasion but not cg1798157 for predicting 1-year and 2-year OS (Table 5). These results suggested that the high accuracy of the prognostic score in predicting OS can be attributed to cg017998157 methylation level in *BTG2* gene.

4. Discussion

BTG2 is a gene transiently expressed in response to various stimuli. Under the stimulation of DNA damage, growth factor signaling, nutrition restriction, oxidative stress, and other conditions caused by genotoxicity, cellular *BTG2* expression can be significantly up-regulated through p53, Ras, STAT3, NFκB, and other pathways, thereby promoting cell death or survival. Thus, *BTG2* is accepted as a mediator of genotoxicity and cellular stress signaling pathways [17]. *BTG2* participates in an array of important biological processes including cell proliferation, autophagy, DNA damage repair, and messenger RNA stability [25–27]. *BTG2* is frequently deleted or mutated in various human malignancies such as lung cancer, prostate cancer, and breast cancer. A decrease in *BTG2* expression is usually indicative of malignant cell behaviors and poor outcomes [19–21]. These findings point *BTG2* towards a tumor suppressor.

DNA methylation is an important epigenetic mechanism essential for regulating gene transcription. Hypermethylation of CpG island in the promoter region of tumor suppressor gene and hypomethylation of whole-genome DNA are critical alterations in carcinogenesis [28]. It is generally believed that hypermethylation of CpG island leads to the silence of tumor suppressor gene. For example, bioinformatics analysis results in non-small cell lung cancer suggest that the DNA methylation level of three CpG sites in *BTG2* (cg01798157, cg06373167, and cg23371584) is negatively correlated with the mRNA expression of BTG2, which is considered a risk factor for overall survival of lung cancer patients [29]. Additionally, the treatment of acute lymphoma cell line Nalm-6 with decitabine (DAC) can cause demethylation of the CpG island in the promoter region of *BTG2* gene and significantly increase its mRNA expression [30]. Of note, down-regulation of *BTG2* gene expression is observed in ICF syndrome (immunodeficiency, centromeric region instability, and facial anomalies caused by DNMT3b mutation), but DNA methylation in the promoter region does not change [31]. Although DAC treatment can elevate the mRNA expression of *BTG2* in breast cancer cell line MCF-7, the CpG island of *BTG2* gene promoter remains an unmethylated state in the cells without DAC treatment [32]. The two studies mentioned above indicate that the expression of *BTG2* may be affected by DNA methylation of other genes in the genome, resulting in the DNA methylation and corresponding mRNA expression of *BTG2* not exhibiting the classic regulation pattern. Our study demonstrated that the methylation of cg01798157 and cg23371584 was negatively correlated with *BTG2* mRNA in the TCGA-LIHC cohort, but the correlation between *BTG2* protein and DNA methylation failed to be verified in our paraffin samples (data not shown). Moreover, we identified methylation level of cg01798157 of *BTG2* gene as an independent prognostic factor for OS of HCC patients who underwent surgical resection (Table 4). The prognostic efficiency of death risk score consisting of cirrhosis, microvascular invasion, and cg01798157 was superior to that of cirrhosis or microvascular invasion alone, but there was no significant difference in comparison with that of cg01798157. It is indicated that the superior prognostic value of death risk score is mainly attributed to cg01798157, and the DNA methylation of *BTG2* gene can be used as a prognostic marker of HCC in Chinese population.

We noticed that cg01798157 is located in the 3′ untranslated region (3′-UTR) of *BTG2* gene, and TCGA-LIHC data showed that almost all CpG sites (cg12586428, cg10935550) in the promoter region of *BTG2* gene in HCC tissues were unmethylated (Fig. 1). Generally, hypermethylation of CpG island in the promoter region silences gene expression, while gene body methylation is conducive to the elongation of gene transcription by preventing spurious transcription initiation [10,33]. However, the function of DNA methylation in the 3′-UTR remains poorly understood. The 3′-UTR is the non-coding sequence at the end of the last exon of the eukaryotic protein-coding gene, which is transcribed to generate precursor RNA and finally retain in mRNA during eukaryotic transcription [34]. Therefore, we suspect that the effect of DNA methylation in the 3′-UTR on transcription may be similar to that of gene body methylation. For example, a recent study has reported that 3′-UTR DNA methylation in T cells promotes gene expression [35]. Moreover, we analyzed CpG sites related to corresponding gene mRNA expression in the TCGA-LIHC dataset and found that 82.5% of CpG sites positively related to gene mRNA expression were located in the gene body and 6.9% were located in the 3′-UTR. However, 31.7% of CpG sites negatively related to corresponding gene mRNA expression were also located in the gene body (Fig. 6A, B). Besides, in the experiment of transient treatment of HCT116 cells with DAC, it was found that the dynamic changes in gene body DNA methylation were not only positively correlated with the expression of its corresponding gene, but also many CpG sites were negatively correlated with the gene expression [36]. Therefore, the effect of DNA methylation in the gene body or even in the intergenic region on gene expression may depend on the gene it “really” regulates. An investigation into imprinted genes contributes to understanding the role of DNA methylation in the non-promoter region [37,38]. In renal cell carcinoma, DLK1 is inactivated by methylation of a downstream faraway CpG island (over 80000bp), whereas gain of methylation upstream of GTL2, a reciprocal imprinted gene for DLK1, is also a critical epigenetic alteration for the inactivation of DLK1 [39]. Many CpG sites correlated with tumor prognosis are located in the gene body or 3′-UTR [29,40], including cg01798157, a prognostic factor for HCC identified in this study. In the light of these findings, we believe that the prognostic significance of DNA methylation and the alterations in DNA methylation regulatory patterns in cancers are worthy of in-depth explorations.

To our knowledge, this is the first study of *BTG2* methylation in HCC. There are however some limitations in this study. Firstly, we did not use training and validation sets to construct and verify the risk score model consisting of cirrhosis, microvascular invasion, and cg01798157. Secondly, the TCGA-LIHC data mainly come from the European and American populations, and the main risk factors are

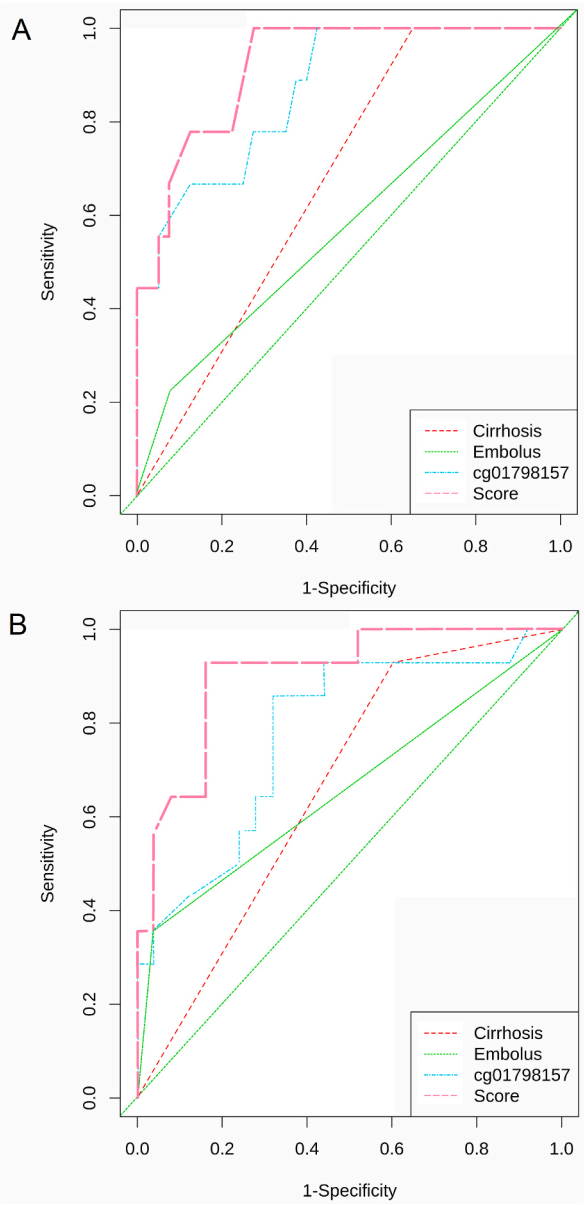

Fig. 5. Time-dependent ROC curves showing predictive accuracy for 1-year [a] and 2-year [b] overall survival rates.

alcohol and hepatitis C. Differences in race and risk factors may lead to different epigenetic profiles of genomes [7]. Our findings may better represent the Chinese population with HCC. Thirdly, due to the small sample size, we failed to carry out stratified analyses on gender, differentiation grading, and Child-Pugh classification of liver function.

5. Conclusions

In summary, the study establishes that the methylation level of cg01798157 in the *BTG2* gene holds significant promise as an epigenetic biomarker for predicting overall survival in Chinese patients with resectable HCC. This methylation was strongly associated with *BTG2* mRNA expression and emerged as an independent prognostic factor for OS, even after adjusting for traditional clinical factors. Moreover, the developed prognostic score based on methylation level, cirrhosis, and microvascular invasion exhibited superior prognostic performance compared to individual clinical factors, as evidenced by higher AUC in time-dependent ROC analysis. This underscores the potential clinical relevance of incorporating *BTG2* methylation levels into prognostic models for HCC, warranting further validation and comparison studies against existing models.

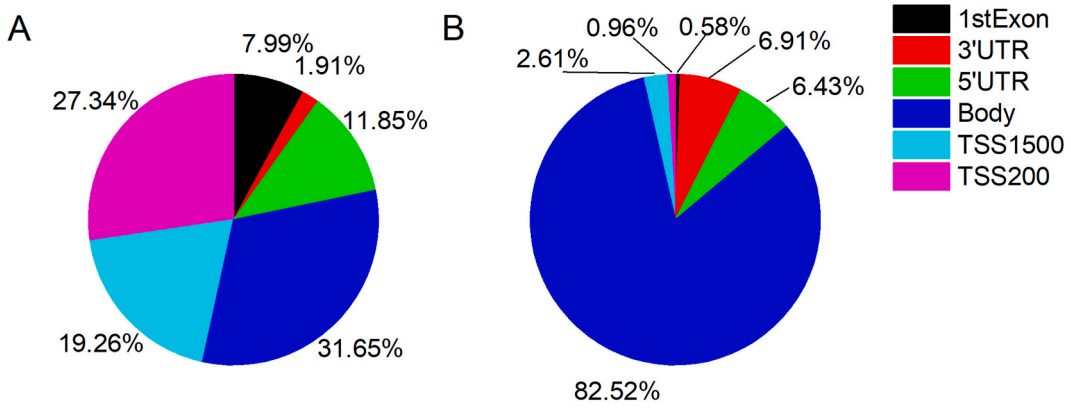

Fig. 6. Pie charts showing distribution of CpG sites significantly associated with *BTG2* mRNA expression in 371 HCC patients in the TCGA HILC dataset. A total number of 2202 and 4170 CpG sites were found to be negatively [a] and positively [b] associated with corresponding gene mRNA expression respectively with the criteria of absolute value of Pearson correlation coefficient greater than 0.5 and adjusted *P* value less than 0.05.

Ethics approval and consent to participate

This study is a retrospective study and all patients' private information had been de-identified.

Data availability statement

The datasets generated and/or analyzed during the current study are available in the preprocessed methylation dataset of liver cancer [(Dataset ID: TCGA.LIHC.sampleMap/HumanMethylation450 version. 2017-09-08); https://xenabrowser.net/datapages/]. The mRNA expression data of 423 tissue samples in the form of $\log_2(x+1)$ transformed from RSEM counts were downloaded from UCSC (https://xenabrowser.net/datapages/).

CRediT authorship contribution statement

Jungang Ma: Conceptualization. **Zhuo Chen:** Formal analysis, Data curation. **Shuixia Liu:** Project administration, Methodology. **Chuan Chen:** Visualization, Validation. **Wei Guan:** Writing – original draft. **Mingying Geng:** Writing – review & editing. **He Xiao:** Supervision. **Bijing Mao:** Formal analysis. **Bin Wang:** Writing – review & editing, Writing – original draft, Methodology, Formal analysis, Conceptualization.

Declaration of competing interest

The authors declare that they have no known competing financial interests or personal relationships that could have appeared to influence the work reported in this paper.

Acknowledgements

We would like to acknowledge the reviewers for their helpful comments on this paper.

List of abbreviations

BTG2	B-cell translocation gene 2
HCC	hepatocellular carcinoma

Appendix A. Supplementary data

Supplementary data to this article can be found online at https://doi.org/10.1016/j.heliyon.2024.e28580.

References

[1] European Association for the Study of the Liver, Electronic address eee European association for the study of the L. EASL clinical practice guidelines: management of hepatocellular carcinoma, J. Hepatol. 69 (2018) 182–236, https://doi.org/10.1016/j.jhep.2018.03.019.

[2] F. Bray, J. Ferlay, I. Soerjomataram, R.L. Siegel, L.A. Torre, A. Jemal, Global cancer statistics 2018: GLOBOCAN estimates of incidence and mortality worldwide for 36 cancers in 185 countries, Ca - Cancer J. Clin. 68 (2018) 394–424, https://doi.org/10.3322/caac.21492.

[3] M. Zhou, H. Wang, X. Zeng, P. Yin, J. Zhu, W. Chen, et al., Mortality, morbidity, and risk factors in China and its provinces, 1990-2017: a systematic analysis for the Global Burden of Disease Study 2017, Lancet 394 (2019) 1145–1158, https://doi.org/10.1016/S0140-6736(19)30427-1.

[4] M. Ueno, S. Hayami, Y. Shigekawa, M. Kawai, S. Hirono, K. Okada, et al., Prognostic impact of surgery and radiofrequency ablation on single nodular HCC ⩽5 cm: cohort study based on serum HCC markers, J. Hepatol. 63 (2015) 1352–1359, https://doi.org/10.1016/j.jhep.2015.07.013.

[5] R.S. Finn, S. Qin, M. Ikeda, P.R. Galle, M. Ducreux, T.Y. Kim, et al., Atezolizumab plus bevacizumab in unresectable hepatocellular carcinoma, N. Engl. J. Med. 382 (2020) 1894–1905, https://doi.org/10.1056/NEJMoa1915745.

[6] P. Tabrizian, G. Jibara, B. Shrager, M. Schwartz, S. Roayaie, Recurrence of hepatocellular cancer after resection: patterns, treatments, and prognosis, Ann. Surg. 261 (2015) 947–955, https://doi.org/10.1097/SLA.0000000000000710.

[7] Cancer Genome Atlas Research Network, Electronic address wbe cancer genome Atlas research N. Comprehensive and integrative genomic characterization of hepatocellular carcinoma, Cell 169 (2017) 1327–1341 e23, https://doi.org/10.1016/j.cell.2017.05.046.

[8] K. Schulze, S. Imbeaud, E. Letouze, L.B. Alexandrov, J. Calderaro, S. Rebouissou, et al., Exome sequencing of hepatocellular carcinomas identifies new mutational signatures and potential therapeutic targets, Nat. Genet. 47 (2015) 505–511, https://doi.org/10.1038/ng.3252.

[9] A. Villanueva, A. Portela, S. Sayols, C. Battiston, Y. Hoshida, J. Mendez-Gonzalez, et al., DNA methylation-based prognosis and epidrivers in hepatocellular carcinoma, Hepatology 61 (2015) 1945–1956, https://doi.org/10.1002/hep.27732.

[10] P.A. Jones, Functions of DNA methylation: islands, start sites, gene bodies and beyond, Nat. Rev. Genet. 13 (2012) 484–492, https://doi.org/10.1038/nrg3230.

[11] Y. Zhang, M. Yang, D.M. Ng, M. Haleem, T. Yi, S. Hu, et al., Multi-omics data analyses construct TME and identify the immune-related prognosis signatures in human LUAD, Mol. Ther. Nucleic Acids 21 (2020) 860–873, https://doi.org/10.1016/j.omtn.2020.07.024.

[12] M. Arora, S. Kumari, J. Singh, A. Chopra, S.S. Chauhan, Expression pattern, regulation, and clinical significance of TOX in breast cancer, Cancer Immunol. Immunother. 70 (2021) 349–363, https://doi.org/10.1007/s00262-020-02689-3.

[13] H. Chen, Q. Qin, Z. Xu, T. Chen, X. Yao, B. Xu, et al., DNA methylation data-based prognosis-subtype distinctions in patients with esophageal carcinoma by bioinformatic studies, J. Cell. Physiol. 236 (2021) 2126–2138, https://doi.org/10.1002/jcp.29999.

[14] J. Qiu, B. Peng, Y. Tang, Y. Qian, P. Guo, M. Li, et al., CpG methylation signature predicts recurrence in early-stage hepatocellular carcinoma: results from a multicenter study, J. Clin. Oncol. 35 (2017) 734–742, https://doi.org/10.1200/JCO.2016.68.2153.

[15] R.H. Xu, W. Wei, M. Krawczyk, W. Wang, H. Luo, K. Flagg, et al., Circulating tumour DNA methylation markers for diagnosis and prognosis of hepatocellular carcinoma, Nat. Mater. 16 (2017) 1155–1161, https://doi.org/10.1038/nmat4997.

[16] E. Dolezal, S. Infantino, F. Drepper, T. Borsig, A. Singh, T. Wossning, et al., The BTG2-PRMT1 module limits pre-B cell expansion by regulating the CDK4-Cyclin-D3 complex, Nat. Immunol. 18 (2017) 911–920, https://doi.org/10.1038/ni.3774.

[17] L. Yuniati, B. Scheijen, L.T. van der Meer, F.N. van Leeuwen, Tumor suppressors BTG1 and BTG2: beyond growth control, J. Cell. Physiol. 234 (2019) 5379–5389, https://doi.org/10.1002/jcp.27407.

[18] F. Tirone, The gene PC3(TIS21/BTG2), prototype member of the PC3/BTG/TOB family: regulator in control of cell growth, differentiation, and DNA repair? J. Cell. Physiol. 187 (2001) 155–165, https://doi.org/10.1002/jcp.1062.

[19] Z. Chen, X. Chen, B. Lu, Y. Gu, Q. Chen, T. Lei, et al., Up-regulated LINC01234 promotes non-small-cell lung cancer cell metastasis by activating VAV3 and repressing BTG2 expression, J. Hematol. Oncol. 13 (2020) 7, https://doi.org/10.1186/s13045-019-0842-2.

[20] V. Coppola, M. Musumeci, M. Patrizii, A. Cannistraci, A. Addario, M. Maugeri-Sacca, et al., BTG2 loss and miR-21 upregulation contribute to prostate cell transformation by inducing luminal markers expression and epithelial-mesenchymal transition, Oncogene 32 (2013) 1843–1853, https://doi.org/10.1038/onc.2012.194.

[21] F. Takahashi, N. Chiba, K. Tajima, T. Hayashida, T. Shimada, M. Takahashi, et al., Breast tumor progression induced by loss of BTG2 expression is inhibited by targeted therapy with the ErbB/HER inhibitor lapatinib, Oncogene 30 (2011) 3084–3095, https://doi.org/10.1038/onc.2011.24.

[22] Y. Chen, C. Chen, Z. Zhang, H. Xiao, B. Mao, H. Huang, et al., Expression of B-cell translocation gene 2 is associated with favorable prognosis in hepatocellular carcinoma patients and sensitizes irradiation-induced hepatocellular carcinoma cell apoptosis in vitro and in nude mice, Oncol. Lett. 13 (2017) 2366–2372, https://doi.org/10.3892/ol.2017.5685.

[23] T. Emura, S. Matsui, V. Rondeau, Survival analysis with correlated endpoints, joint frailty–copula models, in: JSS Research Series in Statistics, Springer, Singapore, 2009, https://doi.org/10.1007/978-981-13-3516-7.

[24] L.M. McShane, D.G. Altman, W. Sauerbrei, S.E. Taube, M. Gion, G.M. Clark, et al., REporting recommendations for tumour MARKer prognostic studies (REMARK), Br. J. Cancer 93 (2005) 387–391, https://doi.org/10.1038/sj.bjc.6602678.

[25] Y. Xu, W. Li, G. Liang, J. Peng, X. Xu, Platelet microparticles-derived miR-25-3p promotes the hepatocyte proliferation and cell autophagy via reducing B-cell translocation gene 2, J. Cell. Biochem. (2020), https://doi.org/10.1002/jcb.29825.

[26] X. Hu, L. Xing, Y. Jiao, J. Xu, X. Wang, A. Han, et al., BTG2 overexpression increases the radiosensitivity of breast cancer cells in vitro and in vivo, Oncol. Res. 20 (2013) 457–465, https://doi.org/10.3727/096504013x13685487925211.

[27] S.S. Hwang, J. Lim, Z. Yu, P. Kong, E. Sefik, H. Xu, et al., mRNA destabilization by BTG1 and BTG2 maintains T cell quiescence, Science 367 (2020) 1255–1260, https://doi.org/10.1126/science.aax0194.

[28] M. Esteller, Cancer epigenomics: DNA methylomes and histone-modification maps, Nat. Rev. Genet. 8 (2007) 286–298, https://doi.org/10.1038/nrg2005.

[29] S. Shen, R. Zhang, Y. Guo, E. Loehrer, Y. Wei, Y. Zhu, et al., A multi-omic study reveals BTG2 as a reliable prognostic marker for early-stage non-small cell lung cancer, Mol. Oncol. 12 (2018) 913–924, https://doi.org/10.1002/1878-0261.12204.

[30] A. Vafadar, P. Mokaram, M. Erfani, Z. Yousefi, A. Farhadi, T. Elham Shirazi, et al., The effect of decitabine on the expression and methylation of the PPP1CA, BTG2, and PTEN in association with changes in miR-125b, miR-17, and miR-181b in NALM6 cell line, J. Cell. Biochem. 120 (2019) 13156–13167, https://doi.org/10.1002/jcb.28590.

[31] A. Jefferson, S. Colella, D. Moralli, N. Wilson, M. Yusuf, G. Gimelli, et al., Altered intra-nuclear organisation of heterochromatin and genes in ICF syndrome, PLoS One 5 (2010) e11364, https://doi.org/10.1371/journal.pone.0011364.

[32] M. Putnik, C. Zhao, J.A. Gustafsson, K. Dahlman-Wright, Global identification of genes regulated by estrogen signaling and demethylation in MCF-7 breast cancer cells, Biochem. Biophys. Res. Commun. 426 (2012) 26–32, https://doi.org/10.1016/j.bbrc.2012.08.007.

[33] F. Neri, S. Rapelli, A. Krepelova, D. Incarnato, C. Parlato, G. Basile, et al., Intragenic DNA methylation prevents spurious transcription initiation, Nature 543 (2017) 72–77, https://doi.org/10.1038/nature21373.

[34] A. Kocabas, T. Duarte, S. Kumar, M.A. Hynes, Widespread differential expression of coding region and 3' UTR sequences in neurons and other tissues, Neuron 88 (2015) 1149–1156, https://doi.org/10.1016/j.neuron.2015.10.048.

[35] M.H. McGuire, S.M. Herbrich, S.K. Dasari, S.Y. Wu, Y. Wang, R. Rupaimoole, et al., Pan-cancer genomic analysis links 3'UTR DNA methylation with increased gene expression in T cells, EBioMedicine 43 (2019) 127–137, https://doi.org/10.1016/j.ebiom.2019.04.045.

[36] X. Yang, H. Han, D.D. De Carvalho, F.D. Lay, P.A. Jones, G. Liang, Gene body methylation can alter gene expression and is a therapeutic target in cancer, Cancer Cell 26 (2014) 577–590, https://doi.org/10.1016/j.ccr.2014.07.028.

[37] D.P. Barlow, Genomic imprinting: a mammalian epigenetic discovery model, Annu. Rev. Genet. 45 (2011) 379–403, https://doi.org/10.1146/annurev-genet-110410-132459.

[38] R. Zwart, F. Sleutels, A. Wutz, A.H. Schinkel, D.P. Barlow, Bidirectional action of the Igf2r imprint control element on upstream and downstream imprinted genes, Genes Dev. 15 (2001) 2361–2366, https://doi.org/10.1101/gad.206201.
[39] T. Kawakami, T. Chano, K. Minami, H. Okabe, Y. Okada, K. Okamoto, Imprinted DLK1 is a putative tumor suppressor gene and inactivated by epimutation at the region upstream of GTL2 in human renal cell carcinoma, Hum. Mol. Genet. 15 (2006) 821–830, https://doi.org/10.1093/hmg/ddl001.
[40] A. Koch, S.C. Joosten, Z. Feng, T.C. de Ruijter, M.X. Draht, V. Melotte, et al., Analysis of DNA methylation in cancer: location revisited, Nat. Rev. Clin. Oncol. 15 (2018) 459–466, https://doi.org/10.1038/s41571-018-0004-4.